ARMY RESEARCH LABORATORY

Characterization of Polyamide 66 Obturator Materials by Differential Scanning Calorimetry and Size-Exclusion Chromatography

by Frederick L. Beyer, Eugene Napadensky, and Christopher R. Ziegler

ARL-TR-3689 **December 2005**

NOTICES

Disclaimers

The findings in this report are not to be construed as an official Department of the Army position unless so designated by other authorized documents.

Citation of manufacturer's or trade names does not constitute an official endorsement or approval of the use thereof.

Destroy this report when it is no longer needed. Do not return it to the originator.

Army Research Laboratory
Aberdeen Proving Ground, MD 21005-5069

ARL-TR-3689 **December 2005**

Characterization of Polyamide 66 Obturator Materials by Differential Scanning Calorimetry and Size-Exclusion Chromatography

Frederick L. Beyer and Eugene Napadensky
Weapons and Materials Research Directorate, ARL

Christopher R. Ziegler
University of Massachusetts, Amherst

REPORT DOCUMENTATION PAGE

Form Approved
OMB No. 0704-0188

1. REPORT DATE *(DD-MM-YYYY)*	2. REPORT TYPE	3. DATES COVERED (From - To)
December 2005	Final	FY04–FY05

4. TITLE AND SUBTITLE
Characterization of Polyamide 66 Obturator Materials by Differential Scanning Calorimetry and Size-Exclusion Chromatography

5a. CONTRACT NUMBER

5b. GRANT NUMBER

5c. PROGRAM ELEMENT NUMBER

6. AUTHOR(S)
Frederick L. Beyer, Eugene Napadensky, and Christopher R. Ziegler*

5d. PROJECT NUMBER
AH80

5e. TASK NUMBER

5f. WORK UNIT NUMBER

7. PERFORMING ORGANIZATION NAME(S) AND ADDRESS(ES)
U.S. Army Research Laboratory
ATTN: AMSRD-ARL-WM-MA
Aberdeen Proving Ground, MD 21005-5069

8. PERFORMING ORGANIZATION REPORT NUMBER
ARL-TR-3689

9. SPONSORING/MONITORING AGENCY NAME(S) AND ADDRESS(ES)

10. SPONSOR/MONITOR'S ACRONYM(S)

11. SPONSOR/MONITOR'S REPORT NUMBER(S)

12. DISTRIBUTION/AVAILABILITY STATEMENT
Approved for public release; distribution is unlimited.

13. SUPPLEMENTARY NOTES
* University of Massachusetts, Amherst

14. ABSTRACT

Samples of two polyamide 6/6 materials used to make obturators were characterized by differential scanning calorimetry (DSC) and by size-exclusion chromatography (SEC). The two materials, commercially available DuPont Zytel 42A and Zytel 101, have been used in obturators, but an increase in undesired part failures occurred when Zytel 101 was replaced with the newer Zytel 42A. DSC analysis of these materials revealed very little variation in the nature of the semicrystalline domains, consistent with a previous analysis using x-ray diffraction. Molecular weight characterization by SEC, however, revealed that the Zytel 101 samples as processed have molecular weights ~10% greater than that of the Zytel 42A samples. The change in molecular weight is reproducible, but contradicts previously collected SEC data from similar samples also from obturator specimens. One factor that is thought to be contributing to the change in molecular weight is the change in the annealing medium from mineral oil to dry nitrogen gas. The apparent variability and significant difference in molecular weight is concluded to be the likely cause of the change in mechanical properties leading to the increased failure rate.

15. SUBJECT TERMS
nylon 66, polyamide, obturator, DSC, SEC, GPC

16. SECURITY CLASSIFICATION OF:			17. LIMITATION OF ABSTRACT	18. NUMBER OF PAGES	19a. NAME OF RESPONSIBLE PERSON
a. REPORT	b. ABSTRACT	c. THIS PAGE			Frederick L. Beyer
UNCLASSIFIED	UNCLASSIFIED	UNCLASSIFIED	UL	24	19b. TELEPHONE NUMBER (*Include area code*) 410-306-0893

Contents

List of Figures

List of Tables

Acknowledgments

Funding for this study was provided by Mr. John Lutz, PM-MAS. The authors would like to acknowledge discussions with Mr. Peter Dehmer in which the effect of annealing media on molecular weight and mechanical properties was jointly developed. The efforts of Mr. Larry Holmes in manufacturing specimens as well as experimental setup were greatly appreciated. Mr. Ziegler was supported by an appointment to the Research Participation Program at the U.S. Army Research Laboratory (ARL) administered by the Oak Ridge Institute for Science and Education through an interagency agreement between the U.S. Department of Energy and ARL.

INTENTIONALLY LEFT BLANK.

1. Introduction

Nylon 6/6, or polyamide 6/6 (PA66), is a semicrystalline, thermoplastic commodity polymer that finds widespread use in applications that require considerable strength but low toughness (Kohan, 1973). One application of PA66 in U.S. Army systems is as an obturator in high-energy kinetic-penetrator rounds. In this application, the PA66 part serves a critical role in the firing of the projectile. The obturator provides the seal between the gun tube and the projectile, allowing the propellant to pressurize the tube behind the round, and guides the projectile smoothly down the barrel. When the round exits the gun tube, the sabots which guided the round down the tube must release the round. Pressure on the obturator from the sabots should cause it to immediately fail, allowing the sabots to separate from each other and release the projectile. Any failure of the obturator either prior to or significantly after the round exits the gun tube will have a detrimental effect on the performance to the round.

The impetus for this study was a change in the failure behavior of PA66 obturators following a change in the stock material used and the manner in which the material was processed. The material was changed from DuPont Zytel 101 to Zytel 42A, and the annealing medium was changed from mineral oil to dry nitrogen gas. The polymer morphology, including crystalline phase, degree of crystallinity, and crystallite orientation, could be affected. The molecular weight averages and distribution may also be affected. These changes have the potential to have a dramatic impact on the physical behavior of the final part. Crystal structure and orientation was previously analyzed and described (Beyer and Ziegler, 2004). In this study, the molecular weight distribution and general variations in crystallinity have been characterized.

The mechanical properties of PA66 can be dramatically influenced by the morphology of the final part, which is in turn influenced by the manufacturing and operating conditions. In the most stable PA66 crystalline structure, the triclinic α-phase, crystallites are comprised of stacks of crystalline sheets (Bunn and Garner, 1947; Cooper et al., 1998; Jones et al., 2000). The sheets are formed by individual PA66 molecules hydrogen-bonded in all-trans conformations. These sheets are not rectangular, but have a slight shear due to a progressive offset between adjacent PA66 chains. Adjacent sheets are also regularly and cumulatively offset, tilting 42° relative the lamellar plane, resulting in a "pleated" crystallite. The second crystalline phase found in PA66, the β-phase, is also triclinic and characterized by sheets that shear alternately in the c-direction, resulting in a 13° offset from the lamellar normal. A third, nonequilibrium crystal phase is observed in PA66 at temperatures near the melting point. The γ-phase, or pseudohexagonal phase, begins to form when PA66 is heated through the "Brill transition." For PA66, the Brill transition temperature (T_B) occurs between 170 °C and 220 °C, well below the melting temperature (T_m), which is in the range of 250 °C to 272 °C (Jones et al., 2000; Pfluger, 1975;

Ramesh et al., 1994). Any change in crystal structure would be expected to have an effect on physical behaviors including toughness and tensile strength.

The molecular weight (MW) distribution of a material will also have a significant impact on its mechanical properties (Kohan, 1973). The MW of nylons is often measured by testing relative viscosity. Increasing relative viscosity, which occurs with increasing MW, correlates with increasing impact toughness and is generally desirable. Increases in crystallinity also improve toughness by providing physical crosslinks. However, in both cases, there is some maximum MW beyond which the effects become detrimental. This maximum depends on the mechanical property, the breadth of the MW distribution, and the specific chemistry of the polymer.

In this study, the two PA66 materials used in the obturators were both characterized by differential scanning calorimetry (DSC) and by size-exclusion chromatography (SEC). DSC allows the analysis of physical changes that affect the absorption and release of heat by the sample, such as melting and glass transitions. The nature and degree of crystallinity of a material may often be obtained from DSC analysis, supporting analysis by other methods. SEC analysis allows the characterization of the MW of the materials, which is a relatively unknown parameter in this particular case due to the in situ polymerization that occurs during extrusion and annealing of the obturator blanks.

2. Experimental

Samples of the two different commercially available nylon materials, DuPont Zytel 101 and Zytel 42A (Wilmington, DE), henceforth "Z101" and "Z42A," were provided by Quadrant Engineering Plastics Products (Reading, PA) at two different stages of the obturator manufacturing process. Both samples were processed according to the recommendations from DuPont, although the exact processing conditions are proprietary. Both materials were extruded at temperatures in excess of 260 °C (500 °F) for several minutes and cooled in a temperature controlled post extrusion die line at a rate of a few in/min. The Z101 materials were then annealed in an industrial-grade mineral oil bath while the Z42A materials were annealed in a dry nitrogen atmosphere, both at ~232.2 °C (450 °F). The annealing time, including ramp up and cool-down time, was ~23 hr. The Z101 sample provided was a large, annealed hollow cylindrical blank. The Z101 blank had an outer diameter of ~5 in and an inner diameter of ~3 in. The Z42A sample was supplied as a fully machined obturator manufactured from a blank similar to the Z101 blank.

To prepare samples for study, wedges were first cut from both the Z42A obturator and Z101 blank using a Felker FRS-51 water-cooled saw (Olathe, KS). Figure 1 shows the geometry of the sections removed from the Z101 blank. Sections were collected in the same manner from the Z42A obturator provided. Water-cooled saws were used to minimize undesirable sample

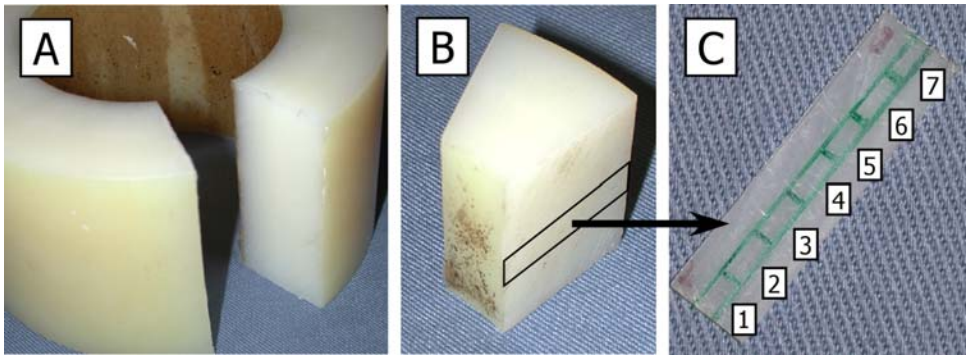

Figure 1. Z101 blank (A) with a large wedge (B) removed. Picture (C) shows a thin section from the wedge with sample locations 1–7 denoted.

heating during preparation. The wedges were then trimmed down to a smaller size so that the wedges fit inside the sample clamp for a low-speed Buehler Isomet 2000 water-cooled diamond saw (Lake Bluff, IL). Using a diamond blade and a cutting speed of ~100 rpm, slices <1 mm thick were taken from the wedges. This thickness was chosen to facilitate the X-ray diffraction analysis, described previously (Beyer and Ziegler, 2004). Multiple slices of Z101 and Z42A were collected in this manner.

For DSC characterization, seven evenly spaced locations along the radial direction of each sample slice were marked, as shown in figure 1. Locations 1, 4, and 7 correspond to the inner surface, the center, and the outer radius of the obturator or blank, respectively. Samples cut from these locations are denoted by Z101-1, Z101-2, etc., indicating both the material and the radial position of the specimen.

Samples weighing ~10 mg each were punched from the slices using a leather punch, weighed, and sealed in aluminum autosampler DSC pans for DSC analysis. DSC analysis was performed using a TA 2920 DSC (TA Instruments, New Castle, DE). The DSC instrument was calibrated using an Indium standard. The procedure for DSC characterization was adapted from PA66 measurements performed by Khanna and Kuhn (1997). After loading each sample into aluminum autosampler pans and crimping the pans closed, a needle was used to create a small hole in the pan lid. The sample was then placed under vacuum at room temperature overnight to dry the sample. After drying, the pan was immediately put into the DSC for a second drying step in which the sample was heated from 25 to ~55 °C at a rate of 20 °C/min, held for 2 min, and then air-cooled to room temperature. The purpose of the second step was to remove additional water and to allow enthalpic relaxations in the amorphous regions of the polyamide that occur as a result of removing moisture during the initial drying step (Khanna and Kuhn, 1997). Khanna and Kuhn found that relaxation of amorphous material causes uncertainty in the baseline above T_g which can lead to incorrect interpretations of crystallinity. After the two drying steps were completed, the sample was heated from 0 to 300 °C at a rate of 20 °C/min and then allowed to

air cool. Specific heat and melt temperature information was obtained through the TA Instruments data acquisition software.

Determining MW of polyamides via SEC is not straight-forward because polyamides are difficult to dissolve in common organic solvents. Concentrated acids, phenol, and fluorinated alcohols are examples of solvents strong enough to dissolve these materials. Using these solvents in standard SEC equipment is very difficult, if not impossible, due to their corrosive properties and toxicity. However, by reacting polyamide with trifluoroacetic anhydride, one can disrupt the intermolecular hydrogen bonding to the point where the polymer will be soluble in common organic solvents, including tetrahydrofuran (THF), a solvent commonly used for SEC. This reaction (given in equation 1) was developed by Schuttenberg and Schulz (Jacobi et al., 1980), and according to Weisskopf and Meyerhoff (1983) does not result in polymer degradation.

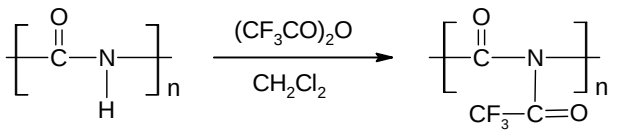

(1)

To perform SEC, small pieces, 19–23 mg each, of both PA66 materials under investigation were cut from the thin slices cut for wide-angle x-ray scattering (WAXS). The samples were taken from the center of the slices since the edges showed some yellowing, often indicative of oxidative degradation. Each sample was placed in a small vial which was then sealed. Using a septum pierced with a syringe, the sealed vials were then purged for 10 min with dry nitrogen. One mL of dichloromethane and 0.1 mL of trifluoroacetic anhydride (~4 molar equivalents as compared to the amount of -NH groups) were then added to both vials. The samples and solvents, sealed in the vials and at room temperature, were stirred overnight, yielding a clear solution. Once clear solutions were available, the vials were opened and the liquids (dichloromethane, trifluoroacetic anhydride, and trifluoroacetic acid) were evaporated out by exposure to a warm bath (40–50 ºC). The residue, N-trifluoroacetylated polyamide, was further dried using dry nitrogen gas, then redissolved in 1 mL of dichloromethane. These solutions were then diluted with 20 mL of THF resulting in solution concentrations of ~1 mg/mL. Each solution was injected into the SEC instrument for analysis after filtration through a 0.45-µm syringe filter. Each solution was prepared immediately prior to analysis in order to minimize aggregation effects and analyzed only twice to ensure that polymer recrystallization would not be an issue.

SEC analyses were performed using a Waters SEC (Waters Corporation, Milford, MA) system composed of a Waters 717-plus autosampler (held at 40 ºC), a Waters 510 pump, a Waters 486 Tunable UV detector set to 254 nm, and a Waters 410 Refractive Index Detector held at 40 ºC. Three columns, a Phenogel 5µ 10^5 Å, a Phenogel 5µ 10^4 Å, and a Phenogel 5µ 10^3 Å (Phenomenex, Rancho Palos Verde, CA), each 300 × 7.8 mm, held at 40 ºC, were used to

separate MWs. The solvent used during this analysis was unstabilized HPLC-grade THF, pumped at a rate of 1 mL/min. Calibration was based on narrow MW polystyrene standards. The injection volume for the polyamides was 50 µL. For polystyrene standards, the injection volume was 100 µL due to lower concentration.

An important issue with N-trifluoroacetylated polyamides is sample stability. Unless the solution is used immediately after preparation, significant changes occur that make MW analysis meaningless. To determine empirically the useful shelf life of the solutions prepared from the PA66 obturator samples, experiments were preformed to observe changes in consecutive SEC chromatograms as the a sample solution aged at 40 ºC. The material used for this analysis was Nylon-6 (20 mg), prepared exactly as just previously described. "Solution age" refers to the time elapsed between the time the solution was made to its injection into the SEC instrument. Examining the overlay of those chromatograms (shown in figure 2), one can see that the retention time of the peak increases with increasing elapsed time. Increasing retention time corresponds to decreasing in molecular weight. Additionally, the area under the peak, which is proportional to amount of polymer detected, decreases, indicating the phenomenon is not simply a decrease in molecular weight due to a reversal of the reaction and loss of the CF_3CO group. Such a reversal would likely produce only a shift in the peak position, not a large decrease in area. The observed shift and decrease in peak area is most likely caused by a decrease in the quantity of sample reaching the detector, and the missing part corresponds to the higher molecular weight portion of the polymer, as implied by the shape of the peaks. Since polymer solution recrystallizes in the solution within 24 hr (Jeon et al., 2004), it is reasonable to assume that the missing higher molecular weight portion of the polymer is forming an insoluble gel that is unable to pass through the SEC column packing. It is interesting to note that the polydispersity of the measured sample seems unaffected by the loss of the high MW fraction.

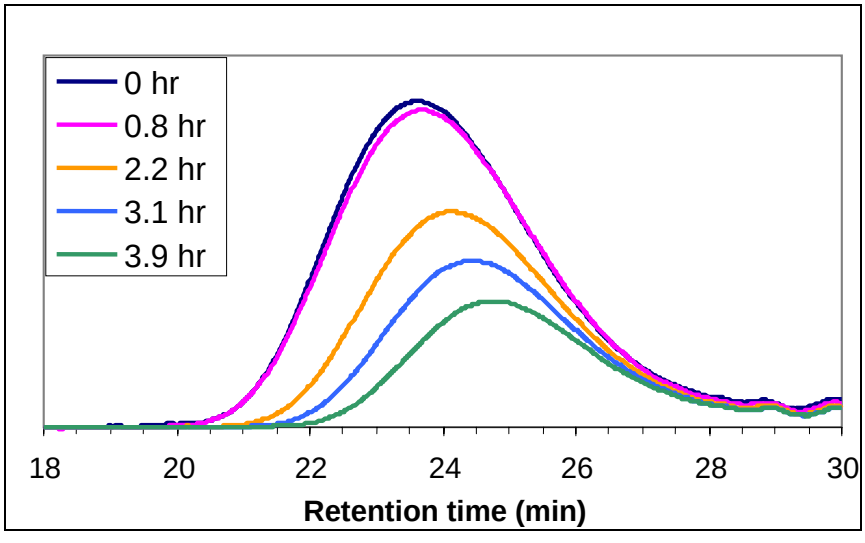

Figure 2. SEC chromatograms showing changes in elution time as the trifluoroacetylated PA66 ages.

For the purposes of this study, it is only important to note that the SEC results remain steady for enough time to allow at least two consecutive measurements of the same sample. Figure 3 supports this conclusion, showing changes in the measured MW and peak area as the samples age, normalized to the data obtained for just-prepared solution (elapsed time = 0). Analyzing samples that are older than one hour would be inadvisable, a situation that was avoided by preparing solutions immediately prior to use.

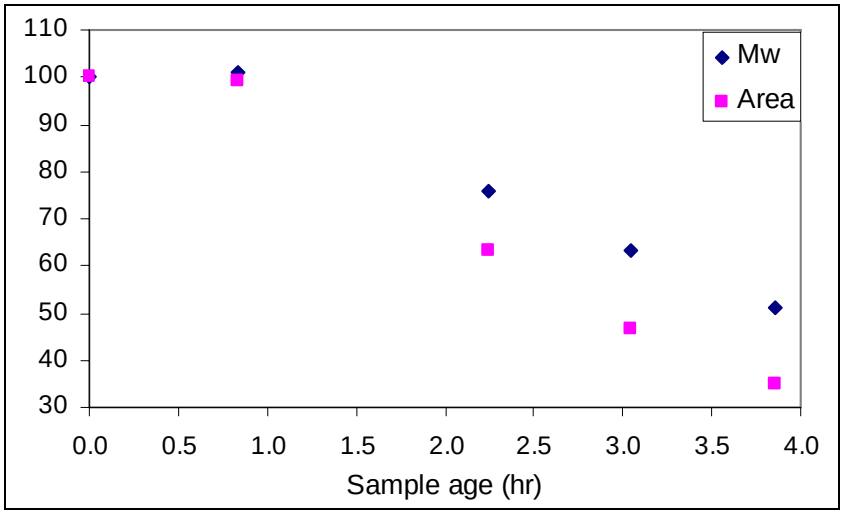

Figure 3. Effect of aging on MW and peak area normalized to the first run.

3. Results

Figure 4 shows examples of typical DSC data collected from PA66 materials Z42A and Z101. In general, DSC data for both PA66 materials Z42A and Z101 have a broad endotherm around ~175 °C and a complex melting endotherm that begins at ~240 °C and ends at ~270 °C. The absence of a crystallization exotherm just above T_g indicates that there is little secondary crystallization occurring in the amorphous regions of the samples. This is expected due to the prolonged annealing regimen employed by the obturator manufacturer and the drying procedure used prior to DSC.

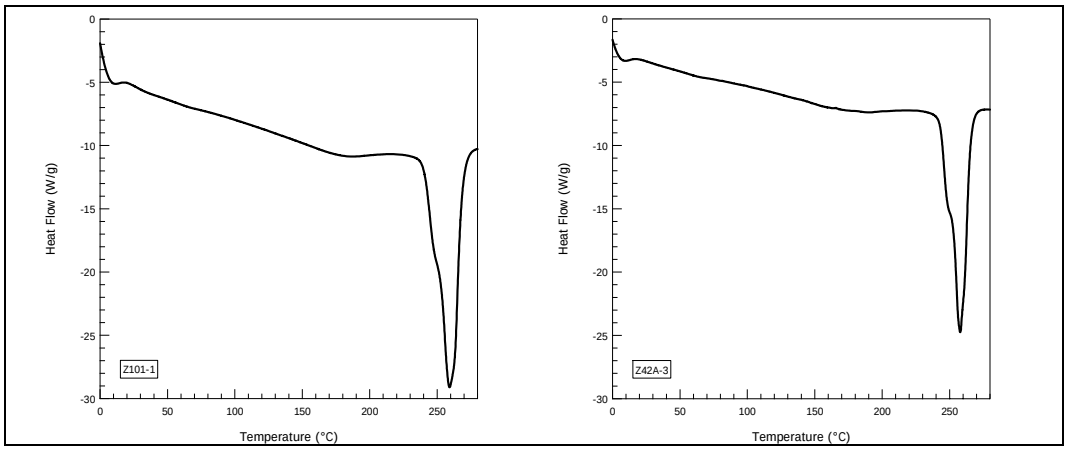

Figure 4. An example of typical DSC data for PA66 Z101 (left) and Z42A (right) materials. As would be expected, the traces are nearly identical.

Figures 5 and 6 show the DSC data collected in the range of the melting endotherm for each of the seven sample locations for the Z101 and Z42A materials, respectively. The breadth of the melting endotherm reveals both α-phase melting and the effects of the Brill transition, in which α-phase crystalline regions transform into the metastable γ-phase (Ramesh et al., 1994; Zhang et al., 2003). What appeared to be one strong endotherm in figure 4 is actually a combination of separate endotherms at 249, 256, and 262 °C. Both materials, Z101 and Z42A, exhibit this behavior. The first peak, at 249 °C, is a result of the melting of α-phase crystallites (Hybart and Platt, 1967; Jones et al., 1997). The high heating rate (20 °C/min) prevents the complete transformation of the α-phase crystallites, around 40% of the bulk of the material (Beyer and Ziegler, 2004), into γ-phase. The two higher temperature peaks comprise a double melting endotherm which results from melting of two different forms of the γ-phase (Zhang et al., 2003). The first peak in the double melting endotherm, "γ_1," seen at 256 °C, is from melting of γ-phase crystallites that are weakly hydrogen bonded. The second peak in the double melting endotherm, "γ_2," which occurs at 262 °C, arises from melting of more strongly hydrogen-bonded γ-phase crystallites.

The results obtained from the SEC analysis are given in figure 7. Both samples were evaluated based on the data collected from the ultraviolet (UV) detector (254 nm) rather than the refractive index detector due to significantly better signal-to-noise ratio. A slight but reproducible shift in retention times between samples can be observed. The stability of the samples is also confirmed; runs "a" were injected immediately after solution preparation, while runs "b" were injected at an elapsed time of 45 min, with no marked differences arising during that period of elapsed time. The calculated MWs derived from the SEC data are given in table 1.

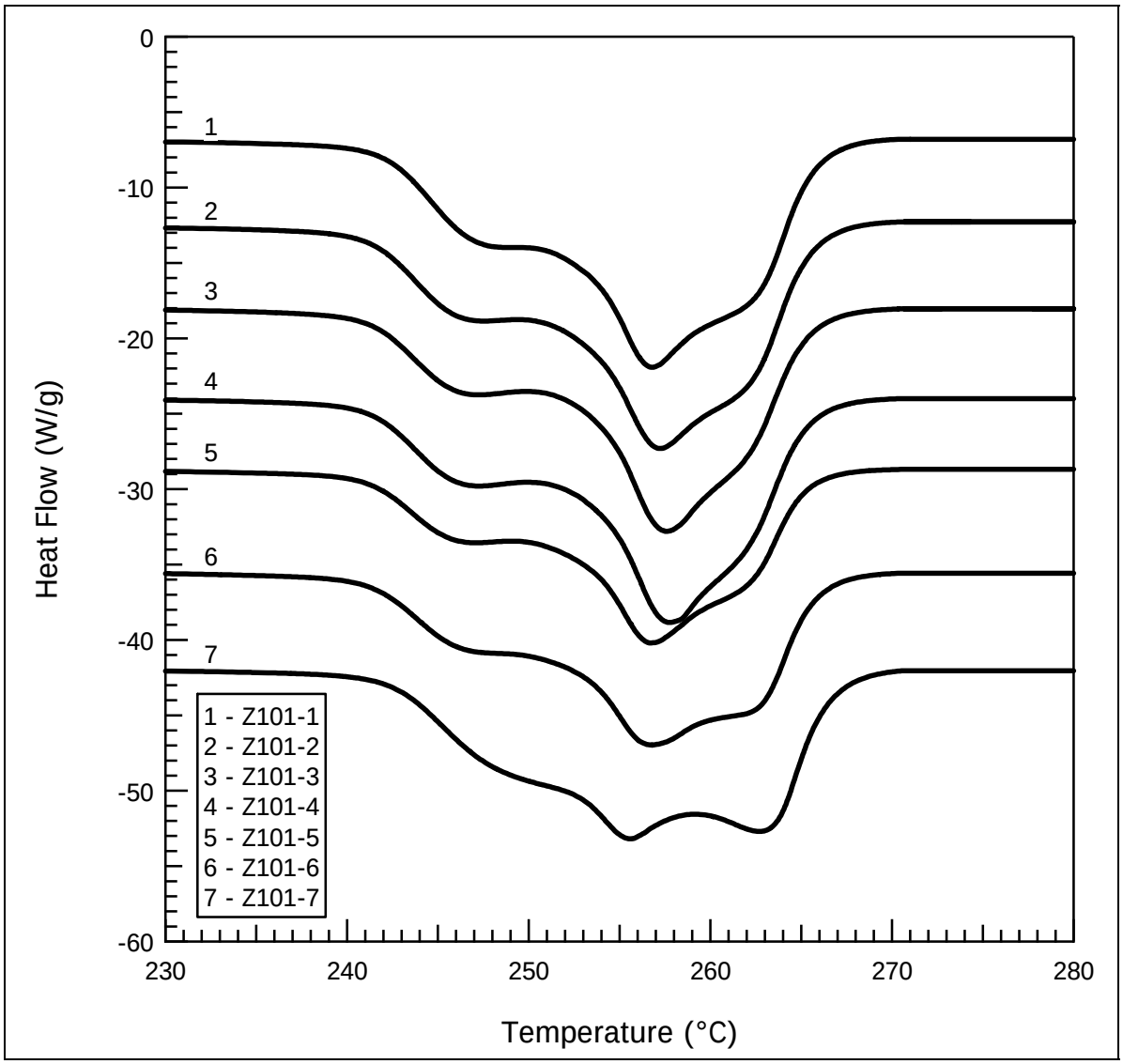

Figure 5. DSC melting endotherms observed for the Z101 samples.

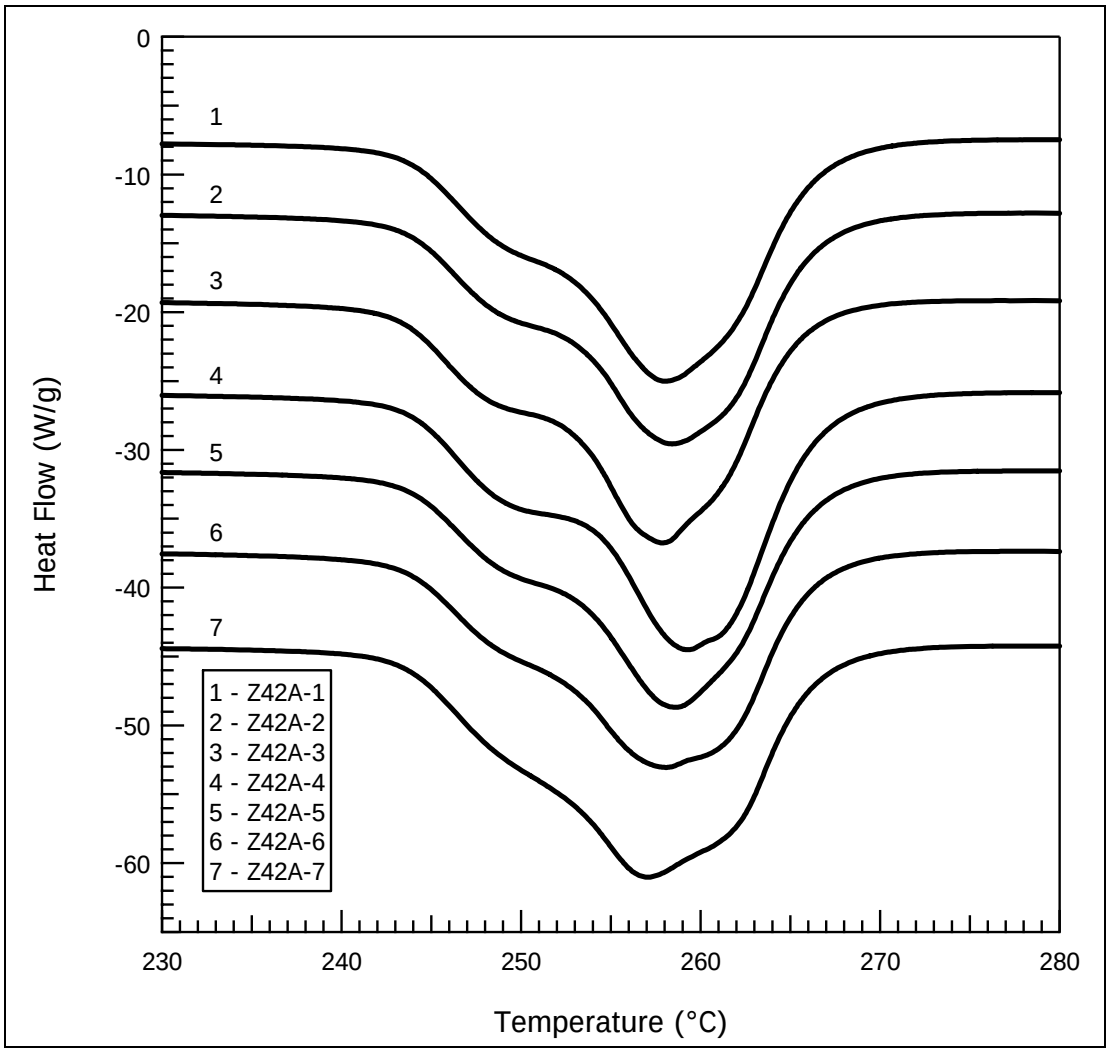

Figure 6. DSC melting endotherms observed for the Z42A samples.

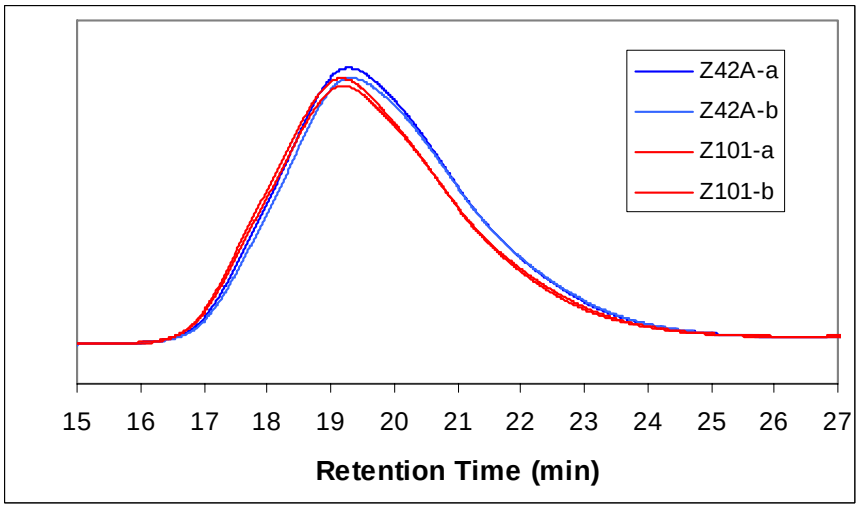

Figure 7. UV-SEC chromatograms of samples Z42A and Z101.

Table 1. SEC results from UV detector (254 nm).

Sample	M_n (g/mol)	M_w (g/mol)	M_z (g/mol)	PDI (M_w/M_n)
Z42A	121,000	233,000	363,000	1.9
Z101	131,000	253,000	390,000	1.9

4. Discussion

In the most general terms, the DSC data collected for both Z101 and Z42A materials can be described as very uniform. This is surely a result of the long annealing process applied to both samples during processing, so that even a large specimen like the blanks has many hours to equilibrate at the annealing temperature. Subtle variations, however, were observed and may correlate to very small differences in morphology within the parts.

The PA66 Z101 DSC data, given in figure 5, show the overall uniformity that arises from the very long annealing process. However, a systematic change in the endothermic peak positions is observed with increasing sample number, or distance from the center of the part. Sample Z101-1 shows a fairly strong α-phase melting peak, a strong γ_1 peak, and a weaker γ_2 peak for strongly hydrogen bonded γ-phase. These data are reasonable when viewed in the context of the earlier WAXS results which indicated minimal γ-phase content, where one would expect a large portion of the γ-phase content to be have formed rapidly, be poorly-organized, and thus weakly hydrogen bonded (Beyer and Ziegler, 2004).

As the outer surface of the part is approached, the relative strengths and positions of the three endotherms vary somewhat. The α-phase melting endotherm stays generally constant until the outer surface is reached (sample Z101-7). The γ_1 peak, however, stays relatively steady until the middle of the part is reached and then begins to shift to a slightly lower temperature and weaken in relative intensity. This weakening is to the benefit of the γ_2 peak, which shifts to a higher temperature and becomes stronger as the outer surface of the part is reached. This behavior seems to indicate an increase in the amount of previously existing γ-phase content at the outer surface of the part. One would expect any γ-phase trapped during the sample cooling process to be more refined in structure, and thus of the stronger hydrogen-bonded type, than that which would form upon heating. Additionally, the shift to a lower temperature of the γ_1 peak would be expected if more of the γ-phase is forming on and around the γ_2 materials. However, the variations in the γ-phase melting endotherms are generally minor, and do not seem to indicate that the Z101 samples contain any significant γ-phase portion prior to heating.

The data for the Z42A samples, shown in figure 6, are very similar overall to that for Z101. A weak endotherm corresponding to melting of α-phase crystallites is observed at ~250 °C. A strong γ_1 endotherm is observed, corresponding to weakly hydrogen-bonded γ-phase crystallites

formed during heating through T_B. A weak γ_2 peak is observed for all samples, indicating a relatively small fraction of more strongly hydrogen bonded γ-phase is present. Some variation in these three melting endotherms is observed, but no consistent trends are developed as they are for the Z101 materials. Samples Z42A-4 shows the most distinct difference from the other sections – a weaker and higher temperature γ_1 endotherm – but in this case, this difference does not seem to be correlated with the γ_2 endotherm, which appears generally weak for all samples.

Analysis of the SEC data given in figure 7 revealed that the actual difference in MW between both samples is not large. The MW for Z101 was ~10% higher that that of Z42A. Polydispersity was found to be identical (~1.9). These data are the results of three separate measurements, which were consistent. It is important to note that the values given in table 1 are not exact because the measured MWs are increased by the addition of trifluoroacetate. The measurements were also made relative to PS standards, which introduces a slight error.

More interesting is the observation that the data given in figure 7 and table 1 directly contradict similar, unpublished data collected by researchers at ATK Thiokol Propulsion on the same materials (Coleman, 2004). In that work, using the same SEC experimental techniques applied in this study, it was found that the MW was ~248.5 kg/mol for the Z101 material and 277 kg/mol for Z42A. The ATK researchers found that the MW averages of the Z42A samples exceeded those of the Z101 materials by ~11.6%, and an average polydispersity measurement was around 2.9 to 3.0, vs. a PDI of 1.9 measured at the U.S. Army Research Laboratory (ARL).

This dramatic difference may have come about in two ways. Human error may have resulted in mislabeled samples or errors in the sample characterization, although every effort was made to ensure correct sample labeling and rigorous adherence to characterization protocol to prevent such basic errors. In this case, though, at least a 10% difference in MW between the two different materials would remain, and the PDIs should be unchanged. Differences in instrumentation and calibration between the ATK and ARL instruments may have some effect on the absolute numbers. Another source of discrepancies could be a very large variation in the MW of the final parts. This idea is not necessarily unrealistic; the Zytel materials as provided by DuPont are not fully reacted and continue to polymerize during the extrusion and annealing process, affecting both MW and polydispersity of the PA66. It is not clear from this study if adequate processing controls were implemented to achieve reproducible MW distributions in either material or by either process.

Regardless of the source of the discrepancies between the ARL and ATK SEC data, both data sets indicate that there is a significant difference of at least 10% in MW between the two materials. Controlling the MW of the materials is critical to controlling physical properties. A high MW clearly could embrittle a sample if it is near the upper limit of the range in which molecular entanglements and physical crosslinks due to crystallinity provide benefit, just as physical properties could be deleteriously affected by a decrease in molecular weight.

One final observation about controlling MW is the role of the annealing medium. The change to a dry nitrogen annealing atmosphere seems very likely to result in a higher molecular weight product simply based on the change in the equilibrium of the polycondensation reaction by which PA66 is made. By annealing in an atmosphere that would readily absorb water, the equilibrium of that reaction would be driven toward the product side of the reaction, increasing MW as water is removed from the reaction medium by the dry nitrogen gas. This effect would not occur for parts annealed in an oil bath, as the solubility of water in oil is minimal.

5. Conclusions

DSC data on the two PA66 materials, Z101 and Z42A, indicate that the samples are virtually indistinguishable with regard to thermal properties. Both materials have triple melting endotherms with nearly identical relative intensities of the three endotherms. Between the two materials, the samples of Z42A showed slightly more consistent thermal behavior while the samples taken from the Z101 part showed some variation in DSC. Specifically, for Z101, variations in the double endotherm for the γ-phase were observed, indicating the possibility of marginally higher γ-phase content near the outer surface of the part.

More importantly, a 10% difference in MW was found between the Z101 and Z42A samples by SEC analysis, with the Z101 sample having the greater MW. This difference is significant, but is not easily explained because it contradicts data previously collected on what are thought to be the same materials. Researchers at ATK Thiokol Propulsion found that the Z42A samples had molecular weights ~12% greater than the Z101 samples. No error in sample characterization, preparation, or labeling could be found that explained this discrepancy. Regardless of the accuracy of either set of SEC data, such a change in MW is significant. More important is the idea that there may be a wide range of possible MWs, and thus mechanical properties, in parts made from these Zytel materials.

Finally, the change in annealing conditions used for parts made from the two materials is likely to affect MW. Specifically, while the parts made from Z101 were annealed in an oil bath, those made from Z42A were annealed in a dry nitrogen atmosphere. The dry nitrogen would rapidly rob the parts of any water, a by-product of the polycondensation polymerization reaction that produces PA66, further increasing the MW of the material. This increase in MW could easily account for the difference in performance properties observed in the field. This idea contradicts the SEC data collected in this study, but is consistent with the results obtained by researchers at ATK.

6. References

Beyer, F. L.; Ziegler, C. *Wide-Angle X-ray Scattering Characterization of the Morphology of Nylon 6 6 Obturator Materials*; ARL-TR-3270; U.S. Army Research Laboratory: Aberdeen Proving Ground, MD, August 2004.

Bunn, C. W.; Garner, E. V. The Crystal Structures of 2 Polyamides (Nylons). *Proceedings of the Royal Society of London Series A-Mathematical and Physical Sciences* **1947**, *189* (1016); p 39.

Coleman, D. W. *GPC Analysis of Nylon*. ATK Alliant Techsystems, Brigham City, UT. Private communication, 2004.

Cooper, S. J.; Atkins, E. D. T.; Hill, M. J. Temperature-Induced Changes in Lamellar Crystals of Monodisperse Nylon 6 and Nylon 6 6 Oligoamides, *Macromolecules* **1998**, *31* (25); 8947–8956.

Hybart, F. J.; Platt, J. D. Melting of 66 Nylon - Observations by Differential Thermal Analysis. *Journal of Applied Polymer Science* **1967**, *11* (8); 1449–1460.

Jacobi, E.; Schuttenberg, H.; Schulz, R. C. A New Method for Gel-Permeation Chromatography of Polyamides, *Makromolekulare Chemie-Rapid Communications* **1980**, *1* (6); 397–402.

Jeon, H. K.; Feist, B. J.; Koh, S. B.; Chang, K.; Macosko, C. W.; Dion, R. P. Reactively Formed Block and Graft Copolymers as Compatibilizers for Polyamide 66/PS Blends, *Polymer* **2004**, *45*; 197–206.

Jones, N. A.; Atkins, E. D. T.; Hill, M. J. Investigation of Solution-Crown, Chain-Folded Lamellar Crystals of the Even-Even Nylons 6 6, 8 6, 8 8, 10 6, 10 8, 10 10, 12 6, 12 8, 12 10, and 12 12. *Journal of Polymer Science Part B-Polymer Physics* **2000**, *38* (9); 1209–1221.

Jones, N. A.; Atkins, E. D. T.; Hill, M. J.; Cooper, S. J.; Franco, L. Chain-Folded Lamellar Crystals of Aliphatic Polyamides. Investigation of Nylons 4 8, 4 10, 4 12, 6 10, 6 12, 6 18, and
8 12. *Polymer* **1997**, *38* (11); 2689–2699.

Khanna, Y. P.; Kuhn, W. P. Measurement of Crystalline Index in Nylons by DSC: Complexities and Recommendations. *Journal of Polymer Science Part B-Polymer Physics* **1997**, *35* (14); 2219–2231.

Kohan, M. I. *Nylon Plastics*; Wiley: New York, NY, 1973.

Pfluger, R. Physical Constants of Nylon 6 and Nylon 66. In *Polymer Handbook*; Brandrup, J., Immergut, E. H., Eds.; John Wiley & Sons: New York, NY, 1975; V66–V79.

Ramesh, C.; Keller, A.; Eltink, S. Studies on the Crystallization and Melting of Nylon 6,6 – 1. The Dependence of the Brill Transition on the Crystallization Temperature. *Polymer* **1994**, *35* (12); 2483–2487.

Weisskopf, K.; Meyerhoff, G. Molecular Weight Determination of Polyamides by N-trifluorocaetylation. *Polymer* **1983**, *24*; 72–76.

Zhang, G. Z.; Watanabe, T.; Yoshida, H.; Kawai, H. Phase Transition Behavior of Nylon-66, Nylon-48, and Blends. *Polymer Journal* **2003**, *35* (2); 173–177.

NO. OF
COPIES ORGANIZATION

1 (PDF ONLY) DEFENSE TECHNICAL INFORMATION CTR
DTIC OCA
8725 JOHN J KINGMAN RD
STE 0944
FORT BELVOIR VA 22060-6218

1 US ARMY RSRCH DEV & ENGRG CMD
SYSTEMS OF SYSTEMS INTEGRATION
AMSRD SS T
6000 6TH ST STE 100
FORT BELVOIR VA 22060-5608

1 INST FOR ADVNCD TCHNLGY
THE UNIV OF TEXAS
AT AUSTIN
3925 W BRAKER LN
AUSTIN TX 78759-5316

1 DIRECTOR
US ARMY RESEARCH LAB
IMNE ALC IMS
2800 POWDER MILL RD
ADELPHI MD 20783-1197

3 DIRECTOR
US ARMY RESEARCH LAB
AMSRD ARL CI OK TL
2800 POWDER MILL RD
ADELPHI MD 20783-1197

3 DIRECTOR
US ARMY RESEARCH LAB
AMSRD ARL CS IS T
2800 POWDER MILL RD
ADELPHI MD 20783-1197

ABERDEEN PROVING GROUND

1 DIR USARL
AMSRD ARL CI OK TP (BLDG 4600)

NO. OF
COPIES ORGANIZATION

1 COMMANDER
US ARMY ARDEC
AMSTA AR CCH P
J LUTZ
BLDG 354
PICATINNY ARSENAL NJ 07806-5000

1 UMASS AMHERST
DEPT OF POLYMER SCI & ENGRNG
C ZIEGLER
120 GOVERNORS DR
AMHERST MA 01003

ABERDEEN PROVING GROUND

14 DIR USARL
AMSRD ARL WM
J SMITH
S MCKNIGHT
AMSRD ARL WM B
J NEWILL
AMSRD ARL WM MA
F BEYER (3 CPS)
E NAPADENSKY (3 CPS)
M VANLANDINGHAM
R JENSEN
L GHIORSE
AMSRD ARL WM MB
W DRYSDALE
AMSRD ARL WM MD
P DEHMER